Co-Synthesis of A Filtering Antenna With Harmonic Suppression

Zhang, Yiming; Zhang, Shuai; Ye, Qi-Cheng; Pedersen, Gert Frølund

Published in:
I E E E Antennas and Wireless Propagation Letters

DOI (link to publication from Publisher):
10.1109/LAWP.2020.3015538

Publication date:
2020

Document Version
Accepted author manuscript, peer reviewed version

Co-Synthesis of A Filtering Antenna With Harmonic Suppression

Yi-Ming Zhang, *Member, IEEE*, Shuai Zhang, *Senior Member, IEEE*, Qi-Cheng Ye, *Student Member, IEEE*, and Gert Frølund Pedersen, *Senior Member, IEEE*

***Abstract*—To suppress the undesired signals at the front-ends of wireless systems, a co-design of a simple filtering antenna highly integrated with a slotline-based network is presented and studied in this letter. The proposed antenna integrated with the low-pass filter, the bandpass response is achieved and impedance bandwidth is also enlarged due to the additional reflection pole contributed by the high integration, which has been evaluated and verified through numerical calculations and full-wave simulations. A design example of the filtering antenna working at 3.5 GHz is developed and fabricated for demonstration purposes. Measured results indicate that good filtering responses with a low insertion loss are achieved. Compared to the original patch antenna, the fractional impedance bandwidth of the proposed one is significantly enhanced, from 6.63% to 13.7%. Besides, harmonics of up to 15.5 GHz are well suppressed. The proposed scheme is simple and compact, exhibiting attractive performance for bandwidth enhancement, and spurious suppression applications.**

***Index Terms*—Harmonic suppression, bandpass, slotline.**

I. Introduction

IT IS of great importance to suppress the undesired frequency bands for antennas in modern wireless communication systems since the harmonic and spurious signals would contribute to the electromagnetic interference and lead to the degradation of communication stability. To address the aforementioned issue, investigations on antennas with filtering responses have attracted increasing attention [1]-[11]. One of the common methods is the employment of antenna-filter fusion approach, where the core is the antenna design with filter-like impedance matching and radiation characteristics [1]-[6]. These studies give the sense that the antenna fusion approach enables the filtering applications for some specified antenna configurations, but might not be feasible for the requirements of using other kinds of antenna types.

Different from the antenna-filter fusion approach, the filter synthesis approach focuses on the integration of antennas and filters, where the antennas are considered as the final loads of the filters. At this point, the design of the filters and the integration of the filters and antennas are the key challenges [7]-[11]. Moreover, the International Telecommunication Union (ITU) [12] and the 3rd Generation Partnership Project (3GPP) [13] give a very strict requirement on out-of-band rejection for industrial applications, where the spurious gain should be at least 43 dB less than the in-band gain. It is very difficult to realize such an attenuation by using only the antenna-filter fusion. Thereby, the investigation of the filter synthesis approach is essential and important.

On the other hand, featuring simple layout, low profile, and low cost, microstrip antennas are most often used at microwave applications [14]. Since both the impedance matching and radiation performance of microstrip patch antennas are sensitive to the physical structures of patch antennas, it is more flexible to use filter synthesis approach. Besides, bandwidth improvement can benefit from the filter synthesis approach [7], [10], and [11], but generally still feature narrow responses.

In this letter, a filtering antenna consisting of a patch and a slotline-based network is proposed and studied under the filter synthesis approach. The filtering network is compact, including a microstrip line loading with four open-circuited stubs and a slotline etched over the microstrip line. Recently, slotline-based microwave components have been studied [15]-[17], but there was no report that a slotline-based low-pass network is proposed for filtering antennas previously. Here, the proposed antenna features a wide harmonic-suppressed band and an improved impedance bandwidth. Moreover, the radiators need to be redesigned in filter synthesis approaches normally, leading to complicated design procedures. As for the proposed design in this letter, the design process is much simpler since the physical sizes of the patch remain unchanged. Only an additional transmission line is pending determination to tune the input impedance of the radiator.

II. Equivalent Circuit Analysis of Proposed Antenna

Shown in Fig. 1 is the configuration of the proposed filtering antenna, consisting of a patch antenna and a slotline-based low-pass filter. Shown in Fig. 1(b) is the bottom view of the physical configuration of the feeding network, including a slotline etched on the ground plane and a microstrip line crossing over the slotline. Four open-circuited stubs are loaded on the microstrip line and symmetrically allocated with respect to the slotline. The characteristic impedance and electrical lengths (referred to the upper edge of the passband, $f_{0,A}$) of the transmission lines of the network are defined as Z_t, Z_s, Z_m, θ_t, θ_s, and θ_m, correspondingly. An additional transmission line with the characteristic impedance and electrical length of Z_a and θ_a

This work was supported by AAU Young Talent Program. (Corresponding author: *Shuai Zhang*)

The authors are with the Antenna, Propagation and Millimeter-wave Systems (APMS) Section, Aalborg University, 9220 Aalborg, Denmark (e-mail: yiming@es.aau.dk; sz@es.aau.dk; qcy@es.aau.dk; gfp@es.aau.dk).

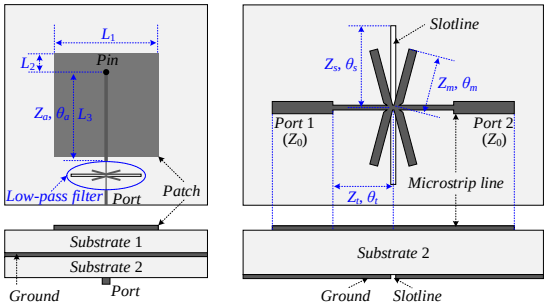

Fig. 1. Configurations of (a) the proposed filtering antenna, and (b) the slotline-based low-pass filter.

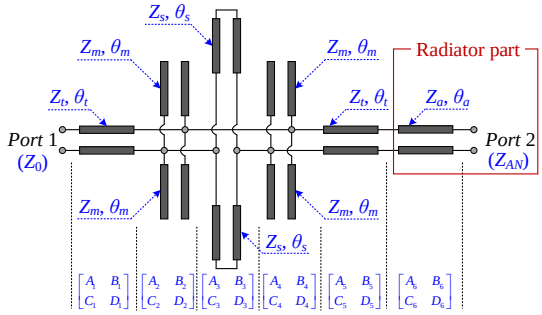

Fig. 2. Equivalent circuit of the proposed filtering antenna.

(referred to $f_{0,A}$), is employed. The line serves as not only the connection between the antenna and the filter but also a key component for impedance matching. Hence, the radiator part includes the patch and the additional transmission line. Fig. 2 shows the equivalent circuit of the filtering antenna given in Fig. 1. The antenna is considered as a two-port network, where the parameter Z_{AN} is the input impedance of the antenna element. The transmission coefficient between ports 1 and 2 represents the transmission performance from Port 1 to free space through the radiator. The circuit is considered the cascade of six sub-network, featured with six transmission matrices. The two subjects of the radiator part are illustrated separately since the values of Z_a and θ_a need to be further determined. Since the input impedance of the radiator part is involved during the synthesis, the patch and the filter are not simply cascaded but a high integration.

As mentioned, the input impedance of a patch antenna is designed with the value of Z_0 at the center frequency (marked as $f_{0,\,AN}$) of the patch antenna, and would change when the frequency departs from $f_{0,AN}$. Here, a fully integrated discussion of the proposed antenna featuring filtering response with improved bandwidth is carried out. Based on the circuit plotted in Fig. 2, the transmission matrix of the two-port circuit model is formulated as [18]

$$\begin{bmatrix} A & B \\ C & D \end{bmatrix} = \begin{bmatrix} A_1 & B_1 \\ C_1 & D_1 \end{bmatrix}\begin{bmatrix} A_2 & B_2 \\ C_2 & D_2 \end{bmatrix}\begin{bmatrix} A_3 & B_3 \\ C_3 & D_3 \end{bmatrix} \times \begin{bmatrix} A_4 & B_4 \\ C_4 & D_4 \end{bmatrix}\begin{bmatrix} A_5 & B_5 \\ C_5 & D_5 \end{bmatrix}\begin{bmatrix} A_6 & B_6 \\ C_6 & D_6 \end{bmatrix} \quad (1)$$

Further, the S parameters of the two-port network shown in Fig. 2 is formulated, expressed as [19]

$$S_{1,1} = \frac{AZ_{AN} + B - CZ_0Z_{AN} - DZ_0}{AZ_{AN} + B + CZ_0Z_{AN} + DZ_0} \quad (2a)$$

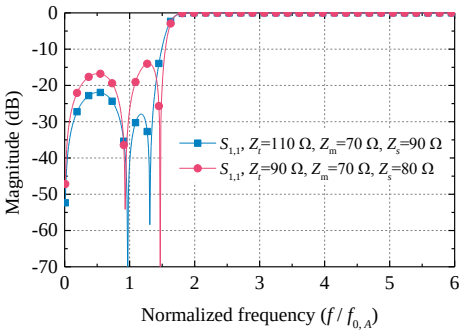

Fig. 3. Calculated results of the slotline-based low-pass filter.

$$S_{2,1} = \frac{2\sqrt{Z_0R_{AN}}}{AZ_{AN} + B + CZ_0Z_{AN} + DZ_0} \quad (2b)$$

where R_{AN} is the real part of Z_{AN}. Next, a numerical study is operated to determine the parameter values of the proposed antenna for filtering, harmonic suppression, and impedance bandwidth improvement purposes. In this case, the following values are utilized that $\theta_t = \theta_m = \pi/8$, $\theta_s = \pi/4$.

Assuming that Z_{AN} and Z_0 always equal to Z_0, the model shown in Fig. 2 becomes the equivalent circuit of the slotline-based low-pass filter. Fig. 3 illustrates some calculated results of the low-pass filter with different parameter values based on (2). It is found that the frequency edges are around $1.5f_{0,A}$. Therefore, it is reasonably concluded that as for the equivalent circuit of the filtering antenna shown in Fig. 2, the realized upper edge of the in-band rang is around $1.5f_{0,A}$, based on the numerical models in (1)-(2). To get a sharp cutoff at the upper frequency edge, it is set that $f_{0,\,AN} = 1.5\ f_{0,\,A}$. Then, impedance matching can be achieved at the frequency $1.5f_{0,A}$, under the following consideration

$$\left(AZ_{AN} + B - CZ_0Z_{AN} - DZ_0\right)\Big|_{f=f_{0,AN}=1.5\,f_{0,A}} = 0 \quad (3)$$

Here, it is defined that

$$Z_a = Z_{AN}\Big|_{f=f_{0,AN}} = Z_0 \quad (4)$$

Substituting (1) and (4) into (3), the numerical relationship between the characteristic impedance Z_t, Z_m, and Z_s can be expressed as

$$Z_s = \frac{P_1' + P_2'}{Q_1' + Q_2'} \quad (5)$$

where

$$P_1' = Z_0^2\left(0.92388Z_tZ_m^2 + 1.84776Z_t^2Z_m\right) \quad (6a)$$

$$P_2' = 0.824954Z_t^4Z_m - 0.92388Z_t^3Z_m^2 \quad (6b)$$

$$Q_1' = Z_0^2\left(0.372583Z_m^2 + 1.490333Z_tZ_m + 1.490333Z_t^2\right) \quad (6c)$$

$$Q_2' = 0.665378Z_t^4 - 1.490333Z_t^3Z_m + 0.834524Z_t^2Z_m^2 \quad (6d)$$

With the given values of Z_t and Z_m, the value of Z_s can be determined. At this point, the S parameters of the two-port network shown in Fig. 2 are determined by Z_t, Z_m, and θ_a, based on (2) and according to (3)-(6). Please note that Z_0 is not the only solution for Z_a, here we use the relation of (4) as a study case. It can be readily verified with different values of Z_a, similar results shown in (5) can always be obtained. The

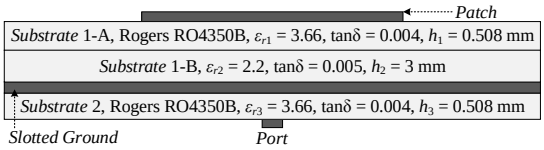

Fig. 4. Side view of the physical structure of the case studied in this work.

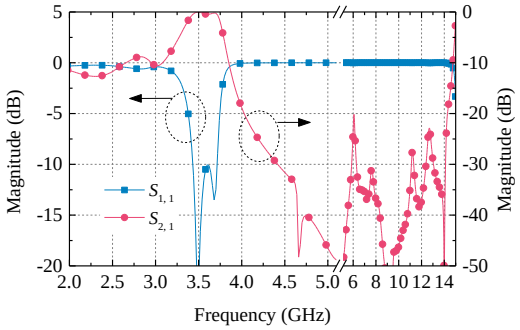

Fig. 5. Calculated transmission responses of the two-port circuit of the filtering antenna, based on the circuit model shown in Fig. 2.

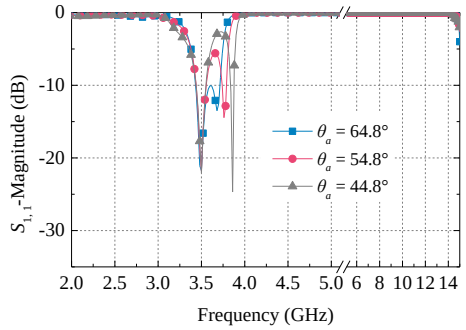

Fig. 6. Calculated $S_{1,1}$ of the two-port circuit of the filtering antenna against different values of θ_a, based on the circuit model shown in Fig. 2

aforementioned discussions focus on the transmission performance at the operating frequency $f_{0,AN}$ of the antenna. As for the out of band, the following determinant is found

$$S_{2,1}\Big|_{f=2f_{0,A}} = S_{2,1}\Big|_{f=4f_{0,A}} = S_{2,1}\Big|_{f=6f_{0,A}} = 0 \qquad (7)$$

It is seen from (7) that for arbitrarily given values of Z_t, Z_m, and Z_s, there would be a transmission zero at the frequencies of $2f_{0,A}$, $4f_{0,A}$, and $6f_{0,A}$, respectively. This implies that a potentially wide-stopband from $2f_{0,A}$ to $6f_{0,A}$ might be achieved for the equivalent circuit. Furthermore, to get a good stopband rejection level, the following condition is employed

$$\left|S_{2,1}\right|_{2f_{0,A}\le f\le 6f_{0,A}} \le -20\,\text{dB} \qquad (8)$$

Finally, a group of specified design parameters can be readily determined on the condition of (8).

For verification purposes, the patch antenna ($f_{0,AN}$ = 3.5 GHz) given in Fig. 1(a) is used as the study case. The practical side view of the patch antenna is illustrated in Fig. 4. A two-stacked-substrate layer is served as the substrate of the patch antenna. The input impedance Z_{AN} of the patch antenna is extracted through full-wave simulations. With the above investigations, the values of Z_t = 98.7 Ω, Z_m = 53.7 Ω, Z_s = 69.1 Ω, $f_{0,LP}$ = 2.333 GHz, and θ_a = 114.3° are theoretically selected, where Z_0 is set as 50 Ω. Fig. 5 shows the calculated transmission responses of the circuit model constructed in Fig. 2, with the derived parameter values. Here, the parameter $S_{2,1}$

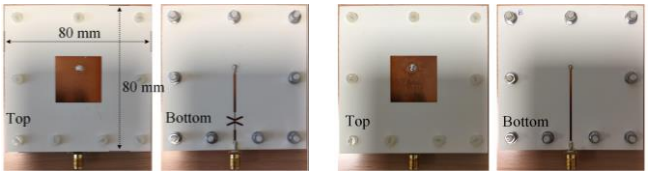

(a) (b)

Fig. 7. Photos of (a) the proposed filtering antenna and (b) the traditional patch antenna.

represents the transmission performance from Port 1 to free space through the radiator. The result denotes that an additional reflection zero is generated, leading to an improved impedance bandwidth. Moreover, transmission zeros are generated at two sides of the passband with good stop rejection, representing a bandpass response. The stopband rejection level of the circuit model implies that for the proposed filtering antenna, a wide harmonic-suppressed band can be achieved. As for the electrical length θ_a, it serves as one of the key parameters for performance improvement, as mentioned before. The influence of θ_a on antenna performance is further discussed based on graphical studies. Fig. 6 depicts the S parameters of the circuit model with different values of θ_a. The result indicates that the value of θ_a has a very small effect on the out-of-band rejection level, but is of great importance to bandwidth enhancement.

To further express the realization of the proposed filtering antenna, a design procedure is summarized as follows:

Step 1: Getting the impedance Z_{AN} of the patch antenna from full-wave simulations.

Step 2: Determining the values of θ_a, Z_t, Z_m, and Z_s based on (5), (6) and (8).

Step 3: Determining the final layout through full-wave simulations.

III. Measurement and Discussion

The filtering antenna centered around 3.5 GHz is further developed and fabricated, as shown in Fig. 7(a). The physical dimensions (width W and length L) of antenna integrated with the feeding network corresponding to Z_t, Z_s, Z_m, Z_a, θ_t, θ_s, and θ_m, are optimized as (unit: mm): W_t = 0.3, W_m = 0.95, W_s = 0.4, W_0 = 1.05, L_t = 4.9, L_m = 5.0, L_s = 9.3. It is clearly seen that the proposed low-pass filter features compactness and simplicity. A traditional patch antenna is also fabricated for comparison purposes, as pictured in Fig. 7(b).

Fig. 8(a) depicts the comparisons of $S_{1,1}$ between the two antennas. For the transitional one, the absolute impedance bandwidth is 240 MHz (6.63%, from 3.50 to 3.74 GHz, referring to $|S_{1,1}| \le -10$ dB), and several reflection nulls are generated from 7 to 15.5 GHz. As for the proposed antenna, the bandwidth is improved to 510 MHz (13.7%, from 3.47 to 3.98 GHz). Two reflection nulls are observed within the passband, which is consistent with the theoretical discussions given in Section II. All the harmonics and other spurious of up to 4.2 times the center frequency of the antenna have been suppressed. Fig. 8(b) and Fig. 8(c) depict the total efficiencies and realized gains of the antennas, respectively. A bandpass response is achieved for the proposed antenna. The in-band total efficiency fluctuates from 77.2% to 84.6%. The realized gain is higher

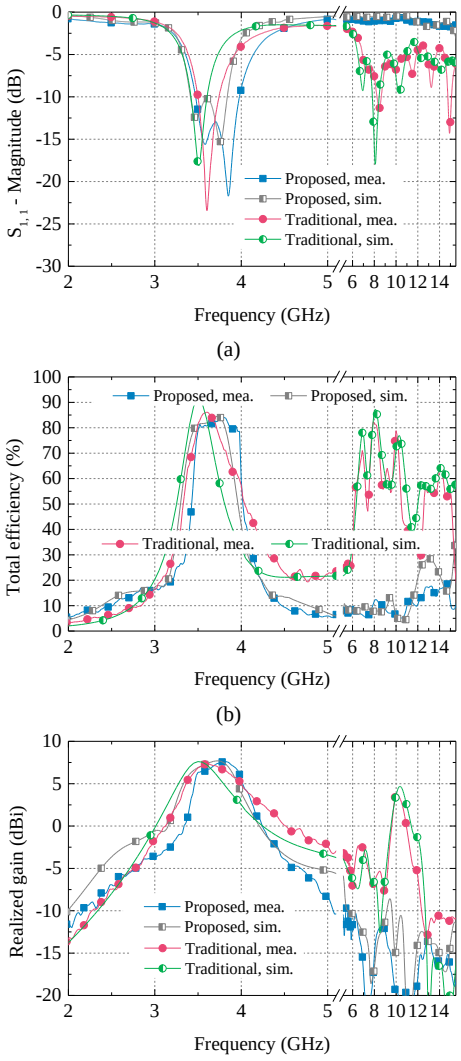

Fig. 8. Measured and full-wave simulated results of the developed filtering antenna and the traditional patch antenna. (a) $S_{1,1}$, (b) total efficiency, and (c) realized gain at boresight.

than 6.14 dBi, with a peak value of 7.65 dBi at 3.8 GHz. Although there is a slight frequency offset between the measured and simulated results owing to the fabrication/assembling errors, good impedance matching and radiation performance are achieved. A quasi-filtering response is observed from the realized gain point of view. The far-field radiation patterns of the proposed filtering antenna are also measured, as described in Fig. 9. Results denote that a low cross-polarization level is obtained within the impedance band.

To further display the performance of the proposed filtering antenna, comparisons with some previously reported filtering antennas are operated, as listed in Table I. As for the proposed filtering antenna, a much wider impedance bandwidth is achieved, compared to most of the mentioned schemes. The harmonics of up to 4.2 times the center frequency are fully suppressed, exhibiting a well-designed harmonic suppression level, with a significant enhancement on impedance bandwidth. As for the spurious rejection level, it was discussed in [20] that it would be difficult to achieve the strict requirement of the ITU

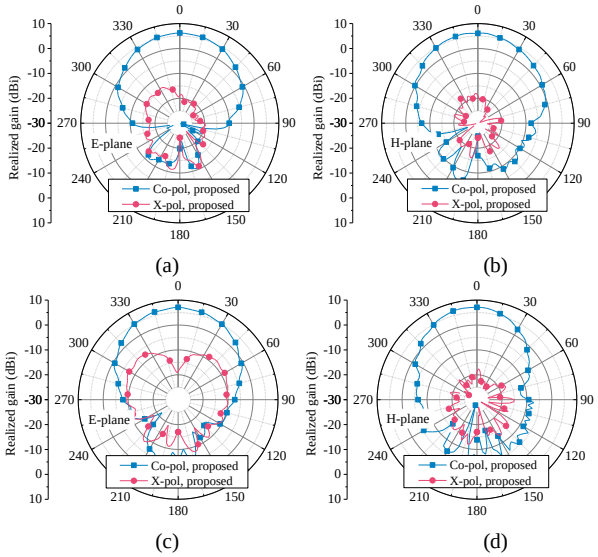

Fig. 9. Measured radiation patterns of the filtering antenna. (a) 3.5 GHz, E-plane. (b) 3.5 GHz, H-plane. (c) 3.9 GHz, E-plane. (d) 3.9 GHz, H-plane.

TABLE I
COMPARISONS BETWEEN SOME PUBLISHED FILTERING ANTENNAS AND THE PROPOSED ONE

Ref.	Antenna scheme	FBW [a]	In-band gain	Spurious rejection
[5]	Element	7.0%	~3.05 dBi	-
[6]	Element	22.6%	~7.4 dBi	$2.3f_0$
[7]	2×2 array	3.0%	≤ 9.6 dBi	-
[8]	Element	6.2%	≤ 6.3 dBi	-
[9]	Element	4.5%	~3.5 dBi	$2.4f_0$
[10]	2×2 array	5.6%	≤ 9.7 dBi	$2f_0$
This work	Element	13.7%	6.14 ~7.65 dBi	$4.2f_0$

[a] denotes the fractional bandwidth.

and 3GPP by only using a single approach (antenna-filter fusion or filter synthesis approaches). For the future, we may center on the investigation of the combination of the two approaches, where the out-of-band rejection performance can benefit from both the radiator and feeding parts.

IV. CONCLUSION

Facing to the demand for the suppression of the undesired frequency bands at antenna level, a filtering antenna integrated with a slotline-based low-pass filtering network is proposed and analyzed for harmonic-suppressed and filtering applications in this letter. Theoretical calculations and full-wave simulations are carried out to verify the performance of the presented structure. A design example is developed and measured. The results demonstrate that for the proposed filtering antenna, the impedance bandwidth is doubled compared to the traditional patch antenna. The proposed scheme is simple and compact with small insertion losses, making it valuable and attractive for harmonic-suppressed and filtering antenna systems.

REFERENCES

[1] C.-X. Mao, S. Gao, Y. Wang, and Z. Cheng, “Filtering antenna with

two-octave harmonic suppression," *IEEE Antennas Wireless Propag. Lett.*, vol. 16, pp. 1361-1364, 2011.

[2] X. He, Y. Zhang, M. Du, and J. Xu, "Lightweight and compact high-gain filtering aperture antenna fabricated by three-dimensional printing technology," *IEEE Antennas Wireless Propag. Lett.*, vol. 17, no. 7, pp. 1141-1144, Jul. 2018.

[3] X. Yang, H. Luyen, S. Xu, and N. Behdad, "Design method for low-profile, harmonic-suppressed filter-antennas using miniaturized-element frequency selective surfaces," *IEEE Antennas Wireless Propag. Lett.*, vol. 18, no. 3, pp. 427-431, Mar. 2019.

[4] C.-W. Tong, H. Tang, J. Li, W.-W. Yang, and J.-X. Chen, "Differentially coplanar-fed filtering dielectric resonator antenna for millimeter-wave applications," *IEEE Antennas Wireless Propag. Lett.*, vol. 18, no. 4, pp. 786-790, Apr. 2019.

[5] P. F. Hu, Y. M. Pan, X. Y. Zhang, and B. J. Hu, "A compact quasi-isotropic dielectric resonator antenna with filtering response," *IEEE Trans. Antennas Propag.*, vol. 67, no. 2, pp. 1294-1299, Feb. 2019.

[6] W. Yang, Y. Zhang, W. Che, M. Xun, Q. Xue, G. Shen, and W. Feng, "A simple, compact filtering patch antenna based on mode analysis with wide out-of-band suppression," *IEEE Trans. Antennas Propag.*, vol. 67, no. 10, pp. 6244-6253, Oct. 2019.

[7] C.-K. Lin, and S.-J. Chung, "A filtering microstrip antenna array," *IEEE Trans. Microw. Theory Tech.*, vol. 59, no. 11, pp. 2856-2863, Nov. 2011.

[8] Y. Yusuf, and X. Gong, "Compact low-loss integration of high-Q 3-D filter with highly efficient antennas," *IEEE Trans. Microw. Theory Tech.*, vol. 59, no. 4, pp. 857-865, Nov. 2011.

[9] Z. H. Jiang, M. D. Gregory, and D. H. Werner, "Design and experimental investigation of a compact circularly polarized integrated filtering antenna for wearable biotelemetric devices," *IEEE Trans. Biomed. Circuits Syst.*, vol. 10, no. 2, pp. 328-338, Apr. 2016.

[10] C.-X. Mao, S. Gao, Y. Wang, Z. Wang, F. Qin, B. Sanz-Izquierdo, and Q.-X. Chu, "An integrated filtering antenna array with high selectivity and harmonics suppression," *IEEE Trans. Microw. Theory Tech.*, vol. 64, no. 6, pp. 1798-1805, Jun. 2016.

[11] F.-C. Chen, H.-T. Hu, R.-S. Li, Q.-X. Chu, and M. J. Lancaster, "Design of filtering microstrip antenna array with reduced sidelobe level," *IEEE Trans. Antennas Propag.*, vol. 65, no. 2, pp. 903-908, Feb. 2017.

[12] "Unwanted emissions in the spurious domain," *Recommendation ITU-R SM.329-12*. https://www.itu.int/rec/R-REC-SM.329/en

[13] "Base Station (BS) radio transmission and reception (Release 16)," *3GPP TS 38.104 V16.2.0*. https://www.3gpp.org/DynaReport/38-series.htm

[14] D. M. Pozar, "Introduction to microwave systems," in *Microwave Engineering*, 4th ed. Hoboken, NJ, USA: Wiley, 2012, ch. 14, pp. 660.

[15] X. Guo, L. Zhu, J.-P. Wang, and W. Wu, "Wideband microstrip-to-microstrip vertical transitions via multiresonant modes in a slotline resonator," *IEEE Trans. Microw. Theory Tech.*, vol. 63, no. 6, pp. 1902-1909, Jun. 2015.

[16] Y.-M. Zhang and J.-L. Li, "A dual-polarized antenna array with enhanced interport isolation for far-field wireless data and power transfer," *IEEE Trans. Veh. Technol.*, vol. 67, no. 11, pp. 10258-10267, Nov. 2018.

[17] Y.-M. Zhang, S. Zhang, J.-L. Li, and G. F. Pedersen, "A dual-polarized linear antenna array with improved isolation using a slotline-based 180° hybrid for full-duplex applications," *IEEE Antennas Wireless Propag. Lett.*, vol. 18, no. 2, pp. 348-352, Feb. 2019.

[18] D. M. Pozar, "Microwave network analysis," in *Microwave Engineering*, 4th ed. Hoboken, NJ, USA: Wiley, 2012, ch. 4, pp. 188-194.

[19] D. A. Frickey, "Conversions between S, Z, Y, H, ABCD, and T parameters which are valid for complex source and load impedances," *IEEE Trans. Microw. Theory Tech.*, vol. 42, no. 2, pp. 205-211, Feb. 1994.

[20] Y.-M. Zhang, S. Zhang, G.-W. Yang, and G. F. Pedersen, "A Wideband Filtering Antenna Array With Harmonic Suppression," *IEEE Trans. Microw. Theory Tech.*, 2020, DOI: 10.1109/TMTT.2020.2993307